Colloids and Surfaces B: Biointerfaces 81 (2010) 249–254

Contents lists available at ScienceDirect

Colloids and Surfaces B: Biointerfaces

journal homepage: www.elsevier.com/locate/colsurfb

Determination of DNA based on localized surface plasmon resonance

Ning Bi, Ying Sun, Hanqi Zhang, Daqian Song, Liying Wang, Jian Wang, Yuan Tian *

College of Chemistry, Jilin University, Changchun 130012, PR China

ARTICLE INFO

Article history:
Received 7 March 2010
Received in revised form 12 June 2010
Accepted 7 July 2010
Available online 13 July 2010

Keywords:
Localized surface plasmon resonance (LSPR)
Resonance light scattering (RLS)
DNA
Gold nanorods

ABSTRACT

A resonance light scattering (RLS) spectrometry for determining DNA based on localized surface plasmon resonance (LSPR) of gold nanorods was developed. The fabrication and characterization of the biosensor utilized gold nanorods as the optical transducer was described. The DNA was determined based on the binding of DNA to gold nanorods by electrostatic adsorption. The RLS intensity of the gold nanorods was enhanced in the presence of DNA. The peaks of the enhanced RLS spectrum were at the wavelength 311 and 581 nm. The binding of DNA to the gold nanorods causes an increase of the RLS intensity that is responsive to the concentration of DNA. Under the optimal conditions, the enhanced RLS intensities are directly proportional to the DNA concentrations in the range of 0.05–0.5 μg/mL. The proposed method was successfully applied to the determination of DNA in the samples and the results were satisfactory.

1. Introduction

Noble metal nanoparticles exhibit a strong absorption band when the incident light frequency is resonant with the collective oscillation of the electrons, which is known as the localized surface plasmon resonance (LSPR) [1–3]. LSPR was employed to detect the immediate change in the interfacial refractive index (RI) of the medium surrounding the nanoparticles. Noble metal nanoparticles are highly sensitive to the RI of their surface bound molecules and surrounding environment, which is the basis of using LSPR for molecular sensing [4]. The increase in RI of the surrounding environment of the noble metal nanoparticles leads to a red shift of the LSPR band, which is greatly affected by the attachment of biomolecules on the nanoparticle surface. The change of RI around the surface of the noble metal nanoparticles can be monitored easily by a scattering or absorption technique. Based on this idea, nano-bio-sensors were designed to detect a small quantity of biomolecules recently [5–7]. Gold and silver nanoparticles are of great interest for label-free sensing because their absorption spectra are highly sensitive to the dielectric constant of the surrounding medium. In addition, the sensitivity to the surrounding medium is strongly depended to the interparticle distance. With the analyte binding on the surface of these nanoparticles, the local RI changes, which thereby provides efficient optical transduction of interfacial binding events [8].

Gold nanoparticles exhibit well-defined optical properties on account of their LSPR phenomena and are developed rapidly and broadly. In aqueous solutions, gold nanoparticles exhibit strong plasmon bands that are depended on their geometric shape and size. The difference between gold nanorods and spherical particles is that gold nanorods appear a surface plasmon band at lower energies and a strong LSPR has been observed [9,10]. For spherical particles, a strong absorption band around 520 nm can be readily observed due to the excitation of plasmon by incident light. Compared to gold nanospheres, the optical and chemical properties of the gold nanorods have some advantages in a quenching and RLS system. For nanorods, two LSPR bands could be observed, one associated with the transverse mode (~520 nm) and the other with the longitudinal mode (usually >600 nm) [11]. The longitudinal plasmon wavelengths are more sensitive to the changes in the dielectric properties of the surroundings and the sensitivity increases with the aspect ratio of the nanorods [12–14]. For the well-defined optical properties, gold nanorods have attracted much attention in biomedical applications such as biosensing, bioimaging and photothermal therapy [15,16].

DNA was often used as a reference for measurements of other parameters in biological samples. And with the number of diseases caused by genetic defects growing, the quantification of DNA is critical to many biological studies. There have been increasing demands for simple, rapid, and reliable methods for the detection of oligonucleotides. At present, there are many determination methods for DNA, including SPR [17], colorimetry [18], fluorescence spectrometry [19] and so on. Meanwhile, there are so many probes for the determination of DNA, such as thidium bromide (EB), diaminobenzoic acid (DABA), diaminophenyl indole (DAPI), cetyltrimethylammmonium bromide (CTAB) [20–22]. Besides these probes, the complexes of trivalent rare earth cations such as Tb(III), Eu(III), La(III), and Y(III)

* Corresponding author. Tel.: +86 431 85168399; fax: +86 431 85112355.
E-mail address: analchem@jlu.edu.cn (Y. Tian).

0927-7765/$ – see front matter © 2010 Elsevier B.V. All rights reserved.
doi:10.1016/j.colsurfb.2010.07.014

[23,24], can be intercalated into the base pair of DNA, resulting in strong fluorescence enhancement due to energy transfer from DNA to the organic dyes. Based on the enhancement effect of resonance light scattering (RLS), the determination of nucleic acids is significantly documented in recent years [20–24]. RLS is a phenomenon of elastic scattering. When the scattering wavelength is near the absorption band of the scattering particles, the light scattering intensity is much higher than the usual light scattering intensity. The RLS spectrum can be easily obtained by simultaneously scanning the excitation and emission monochromators of a common spectrofluorimeter with $\Delta\lambda = 0$ nm [25]. RLS technique has the characteristics of simplicity, quickness and high sensitivity. Most of the RLS methods of determining DNA are based on the RLS intensity change owing to the interaction between DNA and RLS probe. There are many RLS probes for DNA, most of them are the dyes and complexes. The anisotropy of gold nanorods is potentially used as molecular probes for significant changes occur in the plasmon spectra in response to RI changes in the vicinity of the nanorods. Gold nanorods have a great driving force to the development of the method for determining DNA because the method eliminates the need for either organic fluorophores or radioactive labeling.

In this paper, gold nanorods were synthesized by the seed-mediated growth method and positively charged due to the adsorption of the positively charged surfactant CTAB on their surface. Therefore the use of the nanorods simplifies the conjugation with unmodified DNA sequences, which are negatively charged. The LSPR probe can be used to detect the fsDNA by RLS spectrometry. The effect of the interaction of fsDNA and gold nanorods on the RLS intensity was fully investigated. The experimental results indicated that this method exhibited some benefits as sensitivity, simplicity, speediness and stability.

2. Materials and methods

2.1. Materials

Tetrachloroauric acid ($HAuCl_4{\cdot}4H_2O$, 99.99%), sodium borohydride ($NaBH_4$, 99%), silver nitrate ($AgNO_3$, 99%), ascorbic acid (AA, 99.7%), cetyltrimethylammonium bromide (CTAB, 99%) and fish sperm DNA (fsDNA) were purchased from Beijing Ding Guo Biotech. Co. Ltd., China. The fsDNA stock solutions were prepared by dissolving solid fsDNA in doubly distilled water. At least 24 h was needed and occasionally gentle shaking was made for the solutions at 4 °C. H_3PO_4–KH_2PO_4 buffer solution was used to control the acidity of the interaction system. Aqua regia solution (3/1(v/v) HCl/HNO_3) was used to clean the glassware. Other chemicals used here were of analytical reagent grade and all the solutions used in this study were prepared with doubly distilled water.

2.2. Equipments

Absorption spectra were recorded on an Astralian GBC Cintra 10e UV–vis–NIR spectrometer within the wavelength range from 400 to 900 nm. Resonance light scattering experiments were conducted on a Shimadzu RF-5301PC Spectrofluorometer fitted with a xenon lamp using right-angle geometry. The excitation and emission monochromator wavelengths were coupled and adjusted to scan simultaneously within the wavelength range from 220 to 800 nm. The slit widths for the excitation and emission were set as 1.5/1.5 nm. The transmission electron microscope (TEM) image was obtained with a Hitachi H 800 transmission electron microscope operated at an accelerating voltage of 200 kV. The samples for TEM images were prepared by dropping the solutions containing gold nanorods or gold nanorod–fsDNA conjugates on the carbon-coated copper grid and drying at room temperature.

2.3. Preparation of gold nanorods

Gold nanorods were prepared by a seed-mediated growth approach reported by El-Sayed [26,27] with slight modification. All glassware used in these preparations was thoroughly cleaned by immersion in aqua regia solution for 24 h and rinsed with doubly distilled water, then oven-dried prior to use.

2.3.1. Preparation of gold seeds

An aqueous solution containing 5.0 mL of 0.02 mol/L CTAB and 5.0 mL of 5×10^{-4} mol/L $HAuCl_4$ were mixed in a round bottom flask. Then, 0.6 mL of ice-cold 0.01 mol/L $NaBH_4$ solutions was added into the solution with continuous stirring. The solution color changed from dark yellow to brownish yellow immediately after adding $NaBH_4$, which indicated the formation of the gold seeds.

2.3.2. Preparation of gold nanorods

3.0 mL of 4 mmol/L $AgNO_3$ solutions was added into 50.0 mL of 0.2 mol/L CTAB solution at 25 °C. Then 50.0 mL of 1 mmol/L $HAuCl_4$ was added into this solution. The two solutions were gently mixed to obtain the growth solution, and 1.05 mL of 0.1 mol/L ascorbic acid was added into the growth solution. Ascorbic acid as a mild reducing agent made the color of the growth solution change from dark yellow to colorless. Then, 0.24 mL of the gold seed solution was added into the growth solution at 27–30 °C. The color of the solution gradually changed within 10–20 min. The temperature of the growth solution was kept constant at 27–30 °C for 24 h to ensure the growth of the gold nanorods complete. The solution was then centrifuged at 14,000 rpm for 20 min twice to remove the excess surfactant CTAB. The obtained gold nanorods were collected and diluted by water until its absorbance at 705.12 nm was equal to 1.000 and the concentration of gold nanorods in the resulting solution was referred to as 1×. The TEM image in Fig. 1(b) indicates that the shape of the gold nanorods is dogbone. The length of the gold nanorods is about 58 ± 5 nm and the diameter of the gold nanorods is about 26 ± 3 nm.

2.4. Determination of fsDNA

In a series of 10 mL colorimetric tubes, 3 mL gold nanorod solution, 500 μL H_3PO_4–KH_2PO_4 buffer agent and an appropriate volume of fsDNA solution were added. A series of solutions containing different concentrations of fsDNA and the same concentration of gold nanorods were prepared. Then, the solutions were diluted to 10 mL with doubly distilled water and mixed thoroughly with gentle shake. After a certain incubation time, all the measurements were made at room temperature. The RLS spectra were obtained by scanning synchronously with the same excitation and emission wavelengths ($\lambda_{ex} = \lambda_{em}$) from 220 to 800 nm. The enhanced RLS intensity is expressed as $\Delta I_{RLS} = I_{RLS} - I^0_{RLS}$. Here I_{RLS} and I^0_{RLS} are the RLS intensities of the system in presence and the absence of fsDNA, respectively. All experiments were performed in triplicate.

3. Results and discussion

3.1. TEM image of gold nanorods

Fig. 1(a) shows the typical nanostructures of gold nanorods. Compared to {1 1 1} facet, CTAB was apt to adsorb in {1 1 0} facet and formed bilayer structure [28,29]. Therefore, the formed bilayer structure by CTAB in {1 1 0} facet prevented gold ions from depositing in this facet and the gold ions were apt to deposit in {1 1 1} facet, which made the dogbone shape gold nanorods be synthesized.

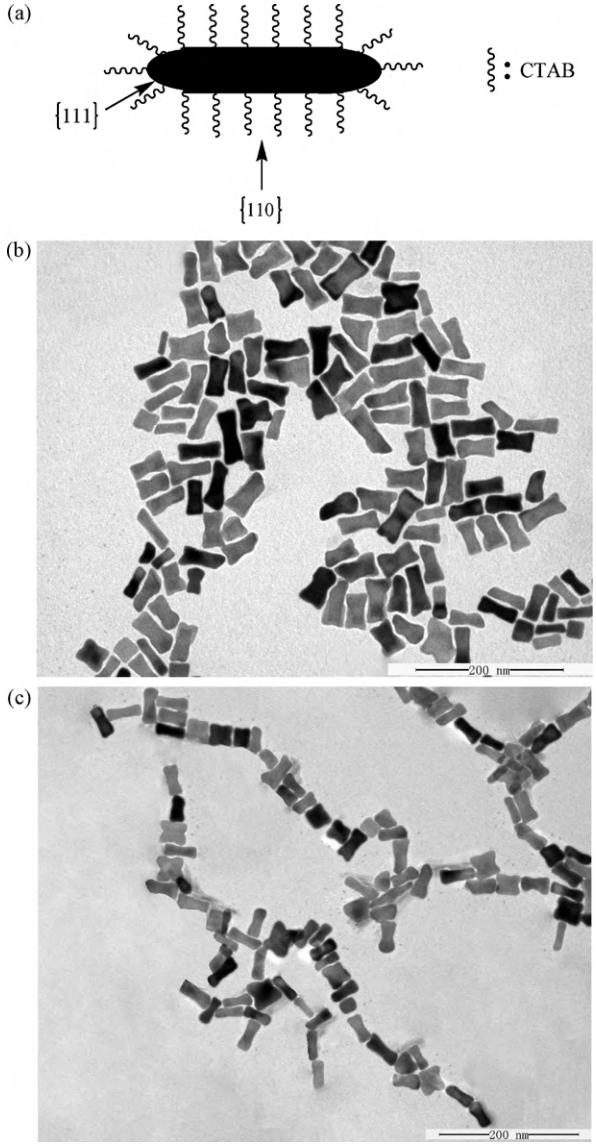

Fig. 1. (a) Nanostructures of the gold nanorod, (b) TEM images of gold nanorods and (c) gold nanorod–fsDNA conjugates.

Fig. 1(b) shows the TEM image of the gold nanorods synthesized by the seed-mediated growth method in the presence of the cation surfactant CTAB. The gold nanorods are positively charged due to the adsorption of the positively charged surfactant CTAB on the surface of the gold nanorods. It is can be seen from Fig. 1(b) that the prepared gold nanorods are of nearly monodisperse and homogeneous. The shape of the gold nanorods is dogbone. The average length of the gold nanorods is about 58 ± 5 nm and the average diameter of the gold nanorods is about 26 ± 3 nm. El-Sayed et al. reported that CTAB molecule formed bilayer structure on the surface of the gold nanorods and has different adsorption ability to different part of the gold nanorods. When the fsDNA was added to gold nanorod suspension, negatively charged DNA adsorbed on the positively charged surfactant CTAB on the gold nanorod surface, which caused the aggregation of gold nanorods. The aggregation has two modes: end-to-end and side-to-side [30,31]. Foss and co-workers said the end-to-end interaction caused a red shift of the longitudinal band that becomes less apparent as the aspect ratio of the rod(s) increases. Conversely, side-to-side interactions of nanorods lead to a blue shift in the main plasmon resonance band with the corresponding growth in the short axis band [32]. Fig. 1(c) shows that the end-to-end interaction plays the main role in this test but the side-to-side interaction also exists.

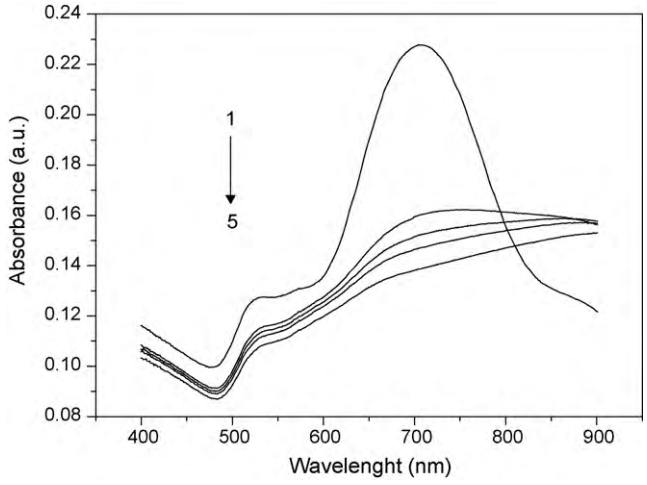

Fig. 2. UV–vis–NIR absorption spectra of gold nanorods in the absence (1) and presence (2–5) of fsDNA for different incubation time: (2) 10 s, (3) 2 min, (4) 5 min and (5) 10 min.

3.2. Optical characterization of gold nanorods

3.2.1. UV–vis–NIR spectrum

Gold nanorods have well-defined optical properties in UV–vis–NIR region. Gold nanorods in aqueous suspension have two distinct plasmon bands that were named the transverse band and the longitudinal band, respectively. The long wavelength plasmon band originates from the longitudinal mode of oscillation of the free electrons along the long axis of the rod, while the short wavelength plasmon band originates from the transverse mode perpendicular to the former one. It is can be seen from Fig. 2 that the gold nanorods before mixed with fsDNA exhibit two well-defined absorption bands, the transverse band located at 533.28 nm and the longitudinal plasmon band at 705.12 nm in UV–vis–NIR spectrum. After mixed with fsDNA solution, the longitudinal band shows a red shift from 705 to 724.32 nm in only 10 s of incubation time and the absorbance decreases significantly. At the same time, the width of the absorption band increases. When the incubation time increases from 2 to 10 min, the longitudinal band shows a red shift from 749.28 to 884.64 nm and the absorbance decreases. Due to the end-to-end interaction between the gold nanorods, the longitudinal band shows a red shift (Fig. 1(c)). Compared to the longitudinal band, the transverse band shows a red shift from 533.28 to 542.88 nm and the absorption peak is weakened gradually. It can be concluded that the longitudinal band is more sensitive than the transverse band.

3.2.2. RLS spectrum

According to the resonance light scattering theory [25,29], the RLS effect is observed as increased scattering intensity at or very near the absorption wavelength of an aggregated molecular species. The effect can be dramatically enhanced when the strong electronic coupling exists among the chromophores. The valuable information on the binding of fsDNA to the surface of the gold nanorods can be obtained from the RLS spectrum. Gold nanorods are the aggregates of Au atoms at nanoscale and their transverse band locates at 533.28 nm (Fig. 2). Therefore, the light scattering peak of gold nanorod–fsDNA system at 581 nm can be characterized as the RLS peak. Fig. 3 shows the light scattering spectra of gold nanorods and the conjugates of gold nanorods at different concentrations of fsDNA in the wavelength range from 220 to 800 nm. It

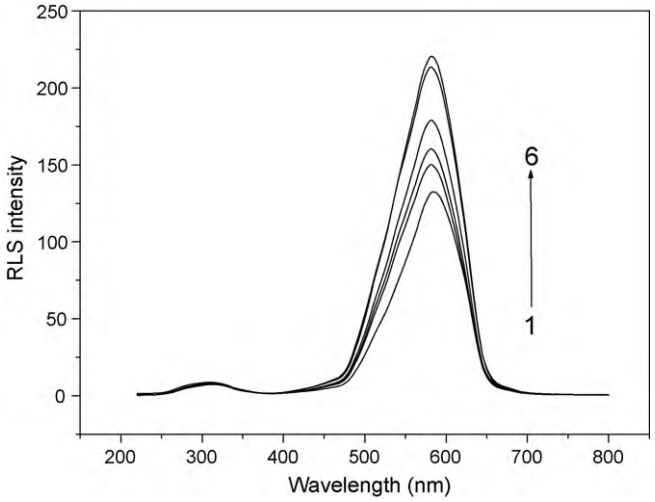

Fig. 3. RLS spectra of gold nanorods in the presence of fsDNA. Concentration of fsDNA: (1) 0 μg/mL, (2) 0.05 μg/mL, (3) 0.1 μg/mL, (4) 0.25 μg/mL, (5) 0.5 μg/mL and (6) 1.0 μg/mL.

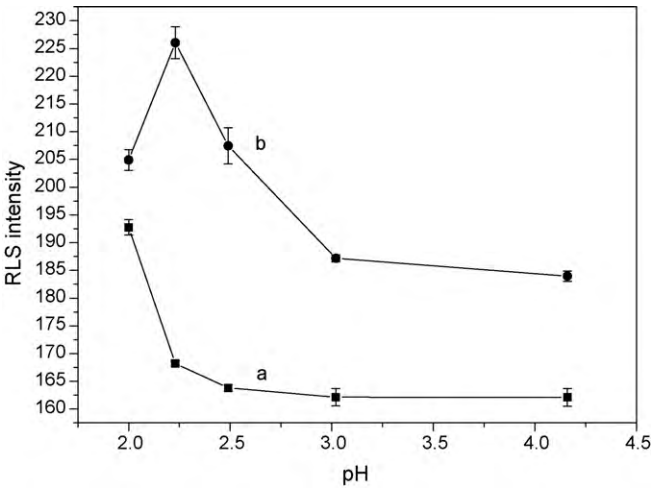

Fig. 4. Influence of pH value on the RLS intensity of gold nanorods (a) and gold nanorod–fsDNA system (b). Concentration of fsDNA, 0.5 μg/mL. Concentration of gold nanorods, 0.3×. Concentration of buffer agent, 5.0 mmol/L.

is can be seen from Fig. 3 that the gold nanorods exhibit two light scattering peaks located at 311 and 584 nm. When a small amount of fsDNA was added into the solution containing gold nanorods, the light scattering peak located at 581 nm is greatly enhanced, while the light scattering peak located at 311 nm is weakened insignificantly. The RLS signals increase with the increasing concentration of fsDNA. At the same time, the RLS wavelength is reduced to 581 nm. It can be concluded that the assembly of gold nanorods and the interparticle plasmons coupling result in great enhancement of RLS of gold nanorods. Additionally, Fig. 1(c) is the TEM image of gold nanorod–fsDNA conjugates that also clearly shows that gold nanorods aggregate with short interparticle distance through the interaction with fsDNA. On the other hand, the assemble of gold nanorods and fsDNA leads to the increase of the size of scatters, which results in the Rayleigh light scattering enhancement in all of the wavelength range from 220 to 800 nm.

3.3. Optimization of experimental conditions

3.3.1. Effect of pH value

The pH values of the solution play an important role in the interaction between gold nanorods and fsDNA. Therefore, the effect of pH values on the RLS intensity was investigated in the pH range from 2.0 to 4.2. The KH_2PO_4–H_3PO_4 buffer solution was used to control the acidity of the analytical solution. As shown in Fig. 4, the RLS signals of the gold nanorods increase with the decrease of pH values. The RLS intensity of gold nanorod–fsDNA conjugates greatly depends on the pH values of the solution and reaches the maximum at pH 2.2. At pH 2.2, by electrostatic interaction, negatively charged fsDNA can easily react with positively charged gold nanorods. Based on the above discussion, pH 2.2 of H_3PO_4–KH_2PO_4 buffer solution was selected to control acidity of the analytical solution.

3.3.2. Effect of the concentration of buffer agent

The effect of the concentration of buffer agent is shown in Fig. 5. With the increase of the concentration of buffer agent, the RLS intensity of the gold nanorods increases. The gold nanorod–fsDNA conjugates produce the maximum RLS intensity at the buffer agent concentration of 5.0 mmol/L, and then the RLS intensity gradually decreases with increasing buffer agent concentration. With the increase of the buffer agent concentration, the concentrations of K^+ and $H_2PO_4^-$ increase and the ionic strength of solution increases, which can influence the electrostatic attraction. Moreover, increasing ionic strength can also slightly induce the aggregation of gold nanorods. The results indicate that a high ionic strength can destroy the electrostatic binding of the gold nanorods with fsDNA. Therefore, the high concentration of the buffer agent was not suitable. Here, 5.0 mmol/L H_3PO_4–KH_2PO_4 buffer solution (pH 2.2) was used to adjust the pH value of solution.

3.3.3. Effect of the concentration of gold nanorods

The concentration of gold nanorods is another important parameter in this method. Fig. 6 shows the effect of the concentrations of gold nanorods on the signals. When the concentrations of the gold nanorods are varied from 0.05× to 0.4×, the RLS intensities increase with the increase of the concentrations of gold nanorods. The shift of RLS intensity reaches the maximum when the concentration of gold nanorods is 0.3×. Therefore, the optimal concentration of gold nanorods was selected as 0.3× for subsequent work.

3.3.4. Effect of the incubation time

The effect of the incubation time on the light scattering intensity of gold nanorods and the gold nanorod–fsDNA system was tested. Fig. 8 shows the change of the RLS intensity with the incubation time. The results show that the reaction between gold nanorods

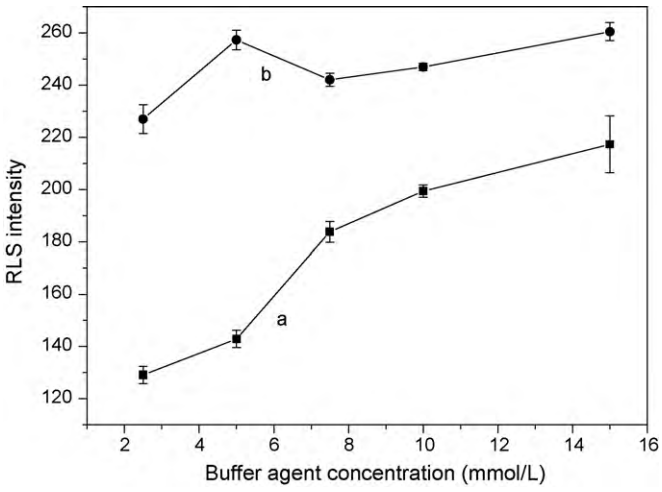

Fig. 5. Effect of buffer agent concentration on the RLS intensity of gold nanorods (a) and gold nanorod–fsDNA system (b). pH, 2.2. Concentration of fsDNA, 0.5 μg/mL. Concentration of gold nanorods, 0.3×.

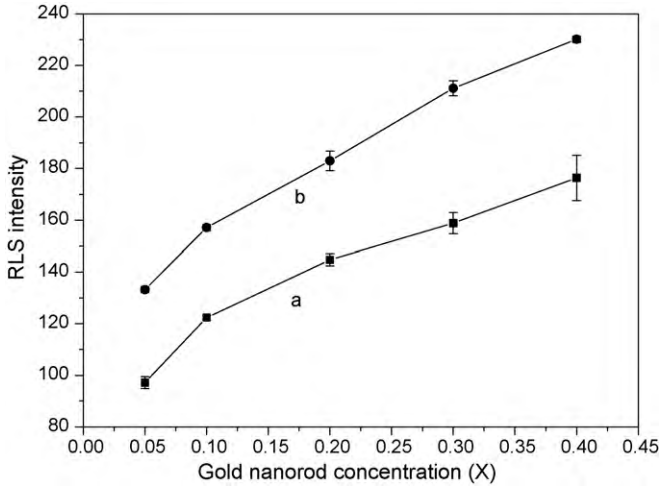

Fig. 6. Influence of gold nanorod concentration on the RLS intensity of gold nanorods (a) and gold nanorod–fsDNA system (b). pH, 2.2. Concentration of fsDNA, 0.5 μg/mL. Concentration of buffer solution, 5.0 mmol/L.

and fsDNA occurs rapidly at room temperature. It can be seen from Fig. 7 that the RLS intensity of system reached a maximum at 2 min and changed slightly until 10 min. After 10 min, the RLS intensity decreases gradually. To make the reaction between gold nanorods and fsDNA complete, all the RLS intensities of analytical solutions were measured at incubation time of 10 min.

3.4. Interference study

Because the fsDNA binding to the gold nanorods was due to electrostatic adsorption, the substances with positive or negative charges will exert an effect on the interaction between the gold nanorods and fsDNA. To study the selectivity for the determination of fsDNA with the proposed RLS method, the RLS responses of various metal ions, sugar and protein were measured according to the general procedure and compared with that of 0.5 μg/mL fsDNA. The effect of some foreign substances on the determination of fsDNA was investigated and the experimental results are listed in Table 1. It can be seen that most of the foreign substances have little influence on the RLS intensity of this system and Na^+, K^+, Ca^{2+}, Mg^{2+} can be allowed with higher concentration levels. Sugar and protein which seem not interact with fsDNA in the optimal conditions and can be allowed at higher concentration levels also. In conclusion, the present assay can be used for the determination of fsDNA in practical samples.

Table 1
Selectivity of the fsDNA assay.

Substance	Concentration ($\times 10^{-6}$ mol/L)	Change of I_{RLS} (%)
Ca^{2+}, Cl^-	100.0	+11.7
Co^{2+}, Cl^-	0.01	−10.3
Cu^{2+}, Cl^-	1.0	−0.8
K^+, Cl^-	200.0	−8.4
Mg^{2+}, Cl^-	100.0	+8.3
Na^+, Cl^-	500.0	−1.2
Zn^{2+}, Cl^-	1.0	−2.1
Glucose	1.0	+12.5
Protein, BSA	0.1[a]	+7.5

[a] Indicate μg/mL.

3.5. Determination of fsDNA

The gold nanorods were synthesized and stabilized by CTAB, which was a powerful surfactant and likely attached only onto the lateral surface of the rods. Under the optimal conditions, different concentrations of fsDNA were detected. ΔI was measured at 581 nm and the dependence of ΔI on fsDNA concentration was established. It is can be seen from Fig. 3 that the RLS intensity is obviously related to concentration of fsNDA. As shown in Fig. 8, ΔI is directly proportional to the fsDNA concentrations in the range 0.05–0.5 μg/mL. The regression equation is $\Delta I = 9.946 + 7.204C$ and the corresponding regression coefficient is 0.998, which indicates that there is a good linear relationship between ΔI and fsDNA concentration.

3.6. Analysis of synthetic samples

To examine the applicability and accuracy of this assay for fsDNA, two synthetic samples containing some foreign substances were analyzed according to the above assay procedure and the experimental results are listed in Table 2. The recovery of analyte in the sample containing Ca^{2+}, K^+, Mg^{2+}, Na^+ is 94.2% and that containing glucose and BSA is 103.8%. The RSDs are less than 2.8%. The results obtained for the synthetic samples indicate that the assay of fsDNA based on LSPR of gold nanorods is sensitive, simple and satisfactory.

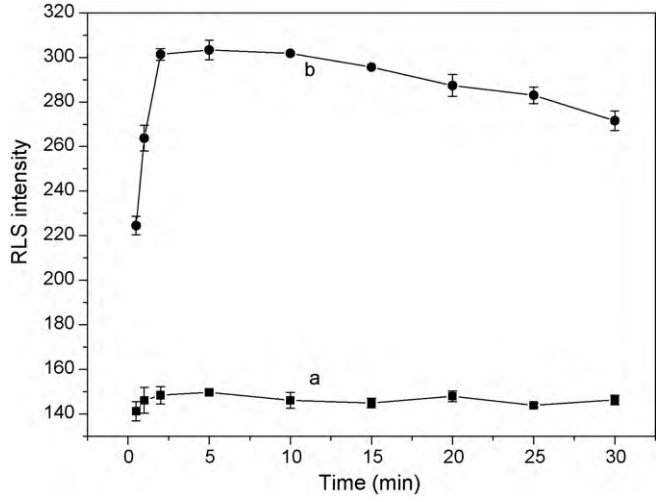

Fig. 7. Effect of incubation time on the RLS intensity of gold nanorods (a) and gold nanorod–fsDNA system (b). pH, 2.2. Concentration of fsDNA, 0.5 μg/mL. Concentration of gold nanorods, 0.3×. Concentration of buffer agent, 5.0 mmol/L.

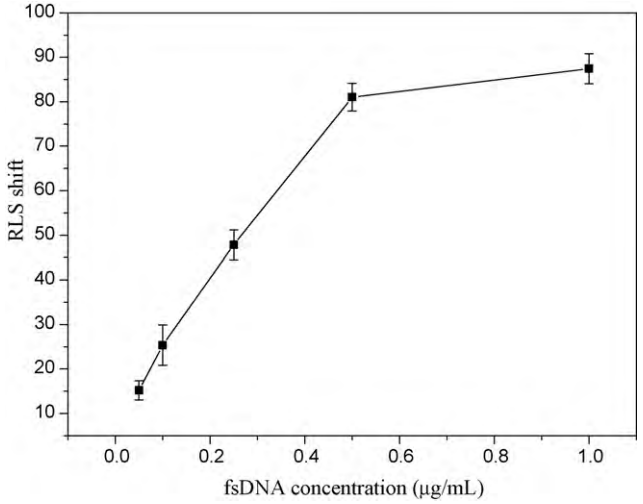

Fig. 8. RLS intensity in dependence on the concentration of fsDNA.

Table 2
Analytical results of synthetic samples.

DNA concentration in sample (μg/mL)	Main additives[a]	Mean concentration found (μg/mL)	Recovery (%)	RSD (%, $n = 3$)
0.50	Ca^{2+}, K^{+}, Mg^{2+}, Na^{+}	0.519	103.8	2.4
0.50	Glucose, BSA	0.471	94.2	2.8

[a] The concentrations of $CaCl_2$, KCl, $MgCl_2$ and NaCl are 10.0×10^{-6} mol/L. The concentrations of glucose and BSA are 0.1×10^{-6} mol/L and 0.05 μg/mL, respectively.

4. Conclusions

Gold nanorods have specific optical characters and were widely used in bioanalysis in recent years. The use of gold nanorods as a probe was investigated for the detection of fsDNA by RLS spectrometry. FsDNA molecules bound to the gold nanorods were detected based on the change of the RLS intensity at the wavelength at 581 nm, which reflects the change in refractive index in the vicinity of gold nanorods. Based on the technology of RLS, the gold nanorods was applied to determining fsDNA with satisfactory results in this assay. At pH value of 2.2, the electrostatic interaction occurs between gold nanorods and fsDNA. The RLS intensity of the gold nanorods is enhanced greatly in the presence of fsDNA, and directly proportional to the concentration of fsDNA. In the application of the LSPR sensing coupled with RLS spectroscopy to the biosensor, this assay has its own merit in convenience and sensitivity and can be adopted to suit the purpose of the detection. The proposed method was applied to the determination of fsDNA in synthetic samples with satisfactory results.

References

[1] K.A. Willets, R.P. Van Duyne, Annu. Rev. Phys. Chem. 58 (2007) 267–297.
[2] H. Huanga, C. Tang, Y. Zeng, X. Yu, B. Liao, X. Xia, P. Yi, P.K. Chu, Colloids Surf. B: Biointerfaces 71 (2009) 96–101.
[3] Y. Sun, Y. Xia, Anal. Chem. 74 (2002) 5297–5305.
[4] J.N. Anker, W.P. Hall, O. Lyandres, N.C. Shah, J. Zhao, R.P. Van Duyne, Nat. Mater. 7 (2008) 442–453.
[5] G. Raschke, S. Kowarik, T. Franzl, C. Sonnichsen, T.A. Klar, J. Feldmann, Nano Lett. 3 (2003) 935–938.
[6] S. Reichelt, K.J. Eichhorn, D. Aulich, K. Hinrichs, N. Jain, D. Appelhans, B. Voit, Colloids Surf. B: Biointerfaces 69 (2009) 169–177.
[7] K.M. Mayer, S. Lee, H. Liao, B.C. Rostro, A. Fuentes, P.T. Scully, C.L. Nehl, J.H. Hafner, ACS Nano 2 (2008) 687–6932.
[8] Z. Mohammed, M. Stephan, R.F. Peter, J.G. Nicholas, Sens. Actuators B: Chem. 94 (2003) 304–312.
[9] M.B. Mohamed, K.Z. Ismail, S. Link, M.A. El-Sayed, J. Phys. Chem. B 102 (1998) 9370–9374.
[10] I. Uechi, S. Yamada, Anal. Bioanal. Chem. 391 (2008) 2411–2421.
[11] J. Perez-Juste, I. Pastoriza-Santos, L.M. Liz-Marz'an, P. Mulvaney, Coord. Chem. Rev. 249 (2005) 1870–1901.
[12] K.S. Lee, M.A. El-Sayed, J. Phys. Chem. B 110 (2006) 19220–19225.
[13] P.K. Jain, S. Eustis, M.A. El-Sayed, J. Phys. Chem. B 110 (2006) 18243–18253.
[14] S. Link, M.A. El-Sayed, J. Phys. Chem. B 109 (2005) 10531–10532.
[15] K.G. Thomas, S. Barazzouk, B.I. Ipe, S.T.S. Joseph, P.V. Kamat, J. Phys. Chem. B 108 (2004) 13066–13068.
[16] X. Huang, I.H. El-Sayed, W. Qian, M.A. El-Sayed, J. Am. Chem. Soc. 128 (2006) 2115–2120.
[17] J. Wang, A. Munir, H.S. Zhou, Talanta 79 (2009) 72–76.
[18] R. Elghanian, J. Storhoff James, C. Mucic Robert, L. Letsinger Robert, A. Mirkin Chad, Science 277 (1997) 1078–1081.
[19] X. Feng, X. Duan, L. Liu, L. An, F. Feng, S. Wang, Langmuir 19 (2008) 12138–12141.
[20] A.I. Kononov, E.B. Moroshikina, J. Phys. Chem. B 105 (2001) 535–541.
[21] J. Rao, W.R. Otto, Fluorimetric D.N.A. assay for cell growth estimation, Anal. Biochem. 207 (1992) 186–192.
[22] Y.F. Li, W. Shu, P. Feng, C.Z. Huang, M. Li, Anal. Sci. 17 (2001) 693–696.
[23] Y.X. Ci, Y.Z. Li, X.J. Liu, Anal. Chem. 67 (1995) 1785–1788.
[24] C.X. Yang, Y.F. Li, C.Z. Huang, Anal. Bioanal. Chem. 374 (2002) 868–872.
[25] R.F. Pasternack, C. Bustmante, P.J. Collings, A. Giannetto, E.J. Gibbs, J. Am. Chem. Soc. 115 (1993) 5393–5399.
[26] B. Nikoobakht, M.A. El-Sayed, Chem. Mater. 15 (2003) 1957–1962.
[27] B. Nikoobakht, M.A. El-Sayed, Langmuir 17 (2001) 6368–6374.
[28] T.K. Sau, C.J. Murphy, Langmuir 21 (2005) 2923–2929.
[29] H.H. Cai, P.H. Yang, J. Feng, J. Cai, Sens. Actuators B: Chem. 135 (2009) 603–609.
[30] Z. Sun, W. Ni, Z. Yang, X. Kou, L. Li, J. Wang, Small 4 (2008) 1287–1292.
[31] M. Sethi, G. Joung, M.R. Knecht, Langmuir 25 (2009) 1572–1581.
[32] M. Gluodenis, C. Foss, J. Phys. Chem. B 106 (2002) 9484–9489.